Transfer learning for CME detection and its application to three-dimensional reconstruction

Jiahui Shan[1,2], Huapeng Zhang [3], Lei Lu[1,2], Yan Zhang[3], **Li Feng** [1,2]

[1]Purple Mountain Observatory, Chinese Academy of Sciences, Nanjing 210023.
[2]School of Astronomy and Space Science, University of Science and Technology of China, Hefei 230026.
[3]State Key Laboratory for Novel Software Technology, Nanjing University, Nanjing 210023.
Contact: lfeng@pmo.ac.cn; shanjh@pmo.ac.cn

Abstract

The SECCHI-COR1 coronagraphs onboard the STEREO have provided extensive polarization observations. Based on the polarization ratio (PR) technique, the three-dimensional coronal mass ejections (CMEs) can be reconstructed. We proposed a method that can automatically derive CME sequences from the mask of the CME region to reconstruct 3-D CMEs. The system can be described in four main steps: classification, segmentation, tracking, and 3-D reconstruction. Considering the high similarity of running-difference images of the SECCHI-COR1 and the SOHO-LASCO C2 coronagraphs, the classification VGG model and the segmentation PSPNet model trained on the data set of LASCO C2 running difference image both are successfully applied to another data set. On the other hand, the method Gradient-weighted Class Activation Mapping (Grad-CAM) interprets that the trained classification model can still focus on the CME region in the SECCHI-COR1 running-difference images. The CME mask part can be obtained by applying a combination of convex hull algorithm and circular filter to the segmented image. For the tracking CME procedure, we adjusted the parameters suitable for COR1, and improved the merging CME regions and velocity fitting. After tracking, the first image of the CME sequence can be used to generate the base polarized brightness (PB) and total brightness (TB). Compared with other PR methods, the mask of the CME region is automatically generated and the results of calculated parameters, such as longitude, latitude, are relatively accurate. A five-year 3D CME catalog of COR1-A is in development. We calculated that the difference in the average start time between the COR1 manual catalog and our catalog is within twenty minutes. In the future, our method can also be adapted to reconstruct the 3-D CMEs from the observations of the Lyman-alpha Solar Telescope (LST) coronagraph onboard the Advanced Space-based Solar Observatory (ASO-S).

Dataset and Method

Data

With the white light observations of the SOHO LASCO C2 coronagraph, we collect running-difference images and categorize them according to their angular width distribution. CME regions are manually marked to create a segmentation dataset (see white structures in Figure 1 a2 & b2). Then, the segmentation model trained on this dataset is applied to the STEREO-A SECCHI COR1 coronagraph observations.

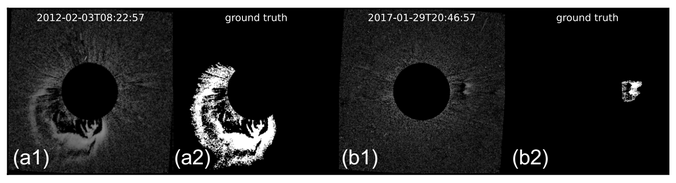

Figure 1. The LASCO C2 running-difference image is paired with the CME mask image it contains.

Method

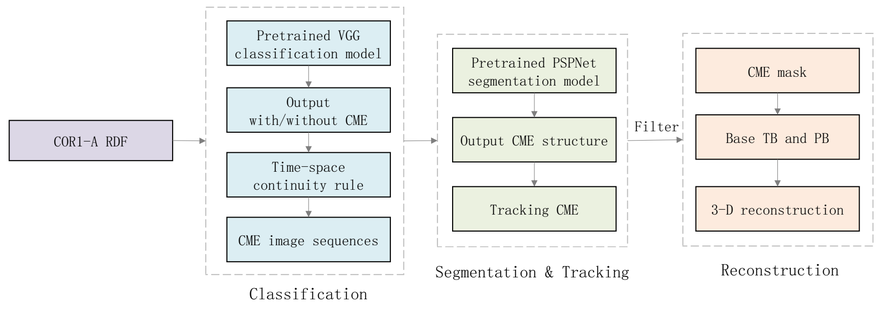

Figure 2. Technology framework for automatic three-dimensional reconstruction of CMEs

Model architecture

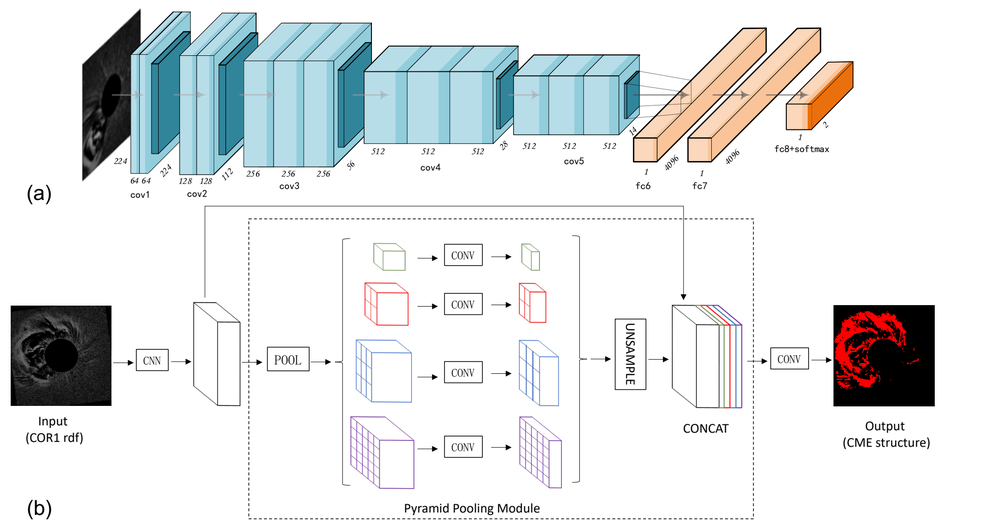

Figure 3. Panel (a) represents the architecture of the VGG classification model. The input to the model is the running-difference images, and the output is two probabilities (with and without CME). Panel (b) shows the PSPNet segmentation model. This model uses running-difference images as input and produces the structure of CMEs as output.

Results

Visualization on CNN features

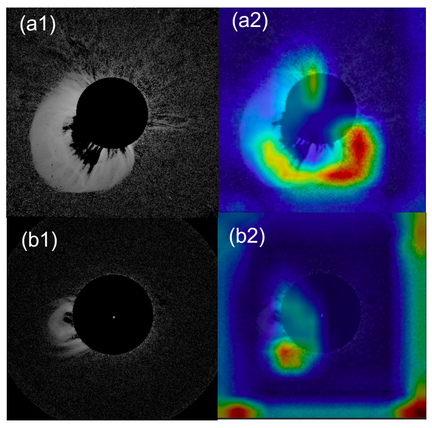

Figure 4. Grad-CAM can be used to visualize the CNN features extracted by VGG from LASCO C2 running-difference images (see panels a2 & b2). As a heat map, Grad-CAM tells us which pixels the model primarily uses to judge the classification. From panel (b2), the orange-red color in the middle of the COR1-A running-difference image also corresponds to the CME region.

Because COR1-A's four corners are all black, some of the corners of the panel (b2) appear dark red. The situation differs from LASCO C2 images but has little impact on the classification result.

Segmentation results and comparison with Wang et al. (2019)

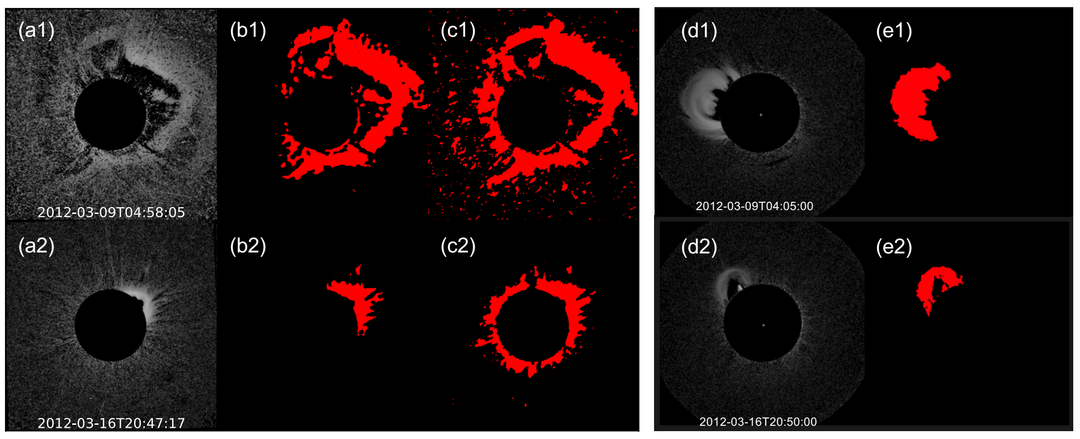

Figure 5. (a) LASCO C2 running-difference images, (b) our PSPNet result, (c) Wang et al. (2019), (d) COR1-A running-difference images, (e) our PSPNet result

In column B and column C of the first row, our method can segment fewer abnormal noise points than Wang et al. (2019). Moreover, as shown in the next row, our method pays more attention to the structure of CMEs. In columns D and E, the segmentation model developed for LASCO C2 is also applicable to STEREO-COR1.

Catalog of COR1-A

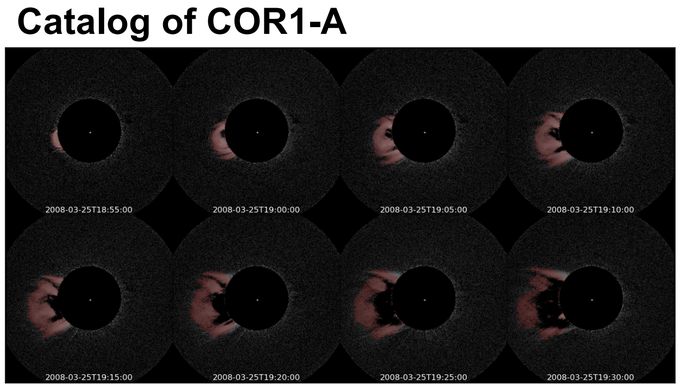

Figure 6. An example of a tracking result, in which the red parts were obtained through segmentation and tracking pipelines applied to CME sequence images.

Year	Detected CME number	Detected CME number in the COR1-A catalog	COR1-A catalog CME number	Accuracy rate(%)	Undetected CME number in the COR1-A catalog
2010	469	322	540	59.630	218
2011	1064	876	1172	74.774	296
2012	1165	929	1192	77.936	263

Table 1. Evaluation of three-year tracking results in comparison with the manual catalog of COR1-A, and calculation of annual recognition rate.

CME 3-D reconstruction

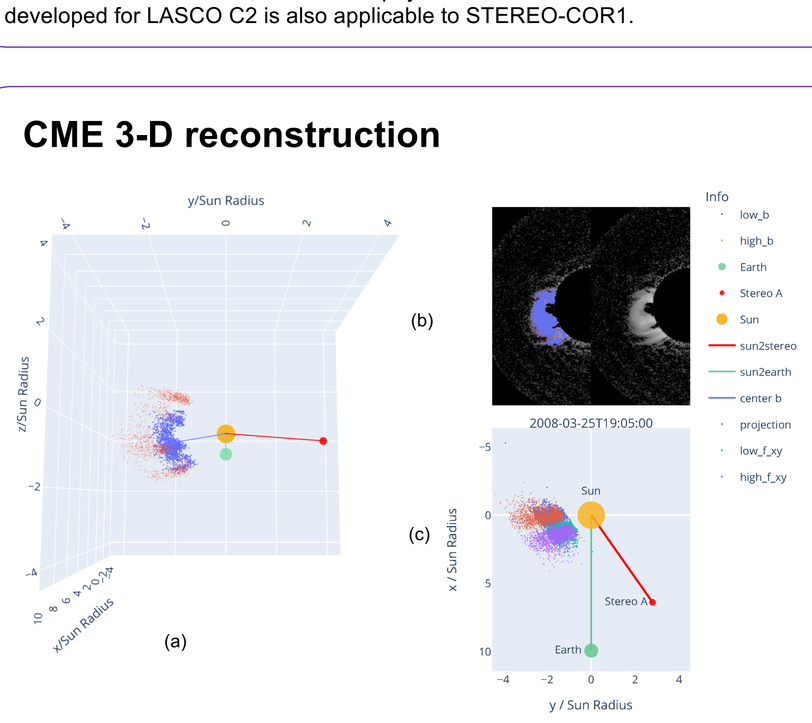

Figure 7. Multi-angle display CMEs in 3-D space. Panel (a) shows the positional relationship between the points of 3-D CME reconstruction on the backside and the sun, the earth, and STEREO-A. In panel (b), blue dots represent 3-D reconstructed points projected onto STEREO-A's total brightness image. Panel (c) is a top view of the panel (a), and the positions of two CMEs on the other side are added.

Time	Method	Fore Lon	Fore Lat	Rcen	Dots Num
2008-03-25T19:05:00	PR base time median 5	-54.956	-13.25	1.886	1881
	PR min bkg median 5	-42.260	-14.720	2.024	9169
	Mierla et al. 2009	-58	-12	1.83	-
2007-08-31T21:30:00	PR base time median 5	79.769	-23.435	2.131	6447
	PR min bkg median 5	67.296	-19.197	2.448	12520
	Mierla et al. 2009	87	-31	1.96	-
2007-05-15T19:15:00	PR base time median 5	-62.885	12.650	2.109	4878
	PR min bkg median 5	-48.538	12.968	2.410	14165
	Mierla et al. 2009	-72	8	2.05	-

Table 2. The parameters of 3-D CME reconstruction are compared with another PR method at three different times.

Conclusions

We propose a method of segmenting the CMEs for the region of interest using deep learning and reconstructing the three-dimensional CME. According to our findings, the classification model and segmentation model trained for LASCO C2 running-difference images could also be applied to COR1-A running-difference images. Furthermore, a five-year 3D CME event catalog is being developed for COR1-A.

- Our segmentation model generates more precise CME structure and reduces the number of abnormal noise points.
- Enhanced tracking algorithm provides more reliable results, like angular width, speed, and height.
- Mask of CMEs generated automatically without the need to manually remove non-CME areas. We are able to reconstruct 3-D CMEs from only one perspective using the PR method.

References

Lu, L., Inhester, B., Feng, L., Liu, S., & Zhao, X. 2017, ApJ, 835, 188
Wang, P., Zhang, Y., Feng, L., et al. 2019, ApJS, 244, 9
Mierla, M., Inhester, B., Marqu´e, C., et al. 2009, SoPh, 259, 123
Zhao, H., Shi, J., Qi, X., Wang, X., & Jia, J. 2017,arXiv:1612.01105